Ecological Indicators 112 (2020) 106085

Contents lists available at ScienceDirect

Ecological Indicators

journal homepage: www.elsevier.com/locate/ecolind

Original Articles

Geostatistical mapping and quantitative source apportionment of potentially toxic elements in top- and sub-soils: A case of suburban area in Beijing, China

Xu-Chuan Duan[a], Hong-Hui Yu[a], Tian-Rui Ye[b], Yong Huang[c], Jun Li[a], Guo-Li Yuan[a,*], Stefano Albanese[d]

[a] School of the Earth Sciences and Resources, China University of Geosciences, Beijing 100083, China
[b] Beijing No. 4 High School International Campus, A2 Xitiejianghutong, Xicheng District, Beijing 100031, China
[c] Beijing Institute of Geo-exploration Technology, Beijing 102218, China
[d] Dipartimento di Science della Terra, dell'Ambiente e delle Risorse, University of Naples Federico II, Napoli 80126, Italy

ARTICLE INFO

Keywords:
Potentially toxic element
Suburban soil
Spatial distribution
Source identification
Risk assessment
Geostatistical map

ABSTRACT

The risk assessment and source identification for potentially toxic elements (PTEs) in soils, particularly agricultural soils from megacities, are significant for environmental protection and pollution control. In this study, an intensive sampling (4127 topsoil samples and 994 subsoil samples) was conducted in the Shunyi District, Beijing, which is a suburban area with extensive cropland cover and has been impacted by the megacity over several decades. Concentrations and distributions of 8 PTEs, including V, Cr, Ni, As, Cd, Zn, Pb and Hg, were determined, and their possible sources were quantitatively assessed by principal component analysis (PCA), redundancy analysis (RDA), positive matrix factorization (PMF) analysis, and anthropogenic contribution ratio method. Among 8 PTEs, Zn, V and Cr exhibited significantly high concentrations in soils, with means of 68.29, 68.19 and 52.13 mg/kg, respectively, followed by Pb (23.84 mg/kg), Ni (22.91 mg/kg), As (8.30 mg/kg), Cd (0.15 mg/kg) and Hg (0.05 mg/kg). RDA and PCA demonstrated that the rock weathering was a significant source of V, Cr, Ni and As, and the local emissions and atmospheric deposition respectively contributed most of Cd, Zn and Pb, and of Hg in soils. This source category was confirmed the spatial variations of anthropogenic contribution ratios to individual PTEs. PMF results showed that the local emissions contributed 96.3% of Cd, 44.4% of Zn and 32.0% of Pb in soils, and the atmospheric source carrying urban pollutants amounted to 78.7–80.2% of Hg. In this case, several effective analysis methods have been successfully applied to quantify the impact of a megacity to PTEs in suburban soils. These results improve understanding of the contamination status of PTEs in suburban soils from Beijing megacity, and provide basis for policymaker regarding environmental protection and pollution control.

1. Introduction

Soil, as an important component of terrestrial ecosystems, plays a crucial role in biochemical transformation, the cycling of elements, and the filtration of water (Luo et al., 2012). It also serves as a reservoir for potentially toxic elements (PTEs), which could be transported from atmosphere, biomass and hydrosphere (Lv et al., 2014). Because of the environmental persistence, high toxicity and great bioaccumulation, the presence of PTEs in soils may threaten ecological safety and endanger the health of organisms through food chain (Akinwunmi et al., 2017; Khan et al., 2008; Lin et al., 2017; Tóth et al., 2016). In addition, PTE exposure could directly reduce immune function through suppressing immune system, as well as through indirect effects to the microbiota, both of which would increase risks from potential diseases (Keesing et al., 2010). Therefore, global concern has been raised over PTE contamination in soils (Chen et al., 2016a; Cortada et al., 2018; Gbadamosi et al., 2018; Ravankhah et al., 2017). Studies focusing on the occurrence and pattern of PTEs in soils would improve understandings for their environmental loads and prediction of human exposure risks.

Both natural and anthropogenic sources could contribute PTEs to soil environment (Yuan et al., 2013). Natural source of PTEs is generally a result of parent rock weathering or pedogenesis (Lin et al., 2017; Wang et al., 2019a), and anthropogenic pollutants are directly

* Corresponding author.
E-mail address: yuangl@cugb.edu.cn (G.-L. Yuan).

https://doi.org/10.1016/j.ecolind.2020.106085
Received 28 August 2019; Received in revised form 29 December 2019; Accepted 6 January 2020

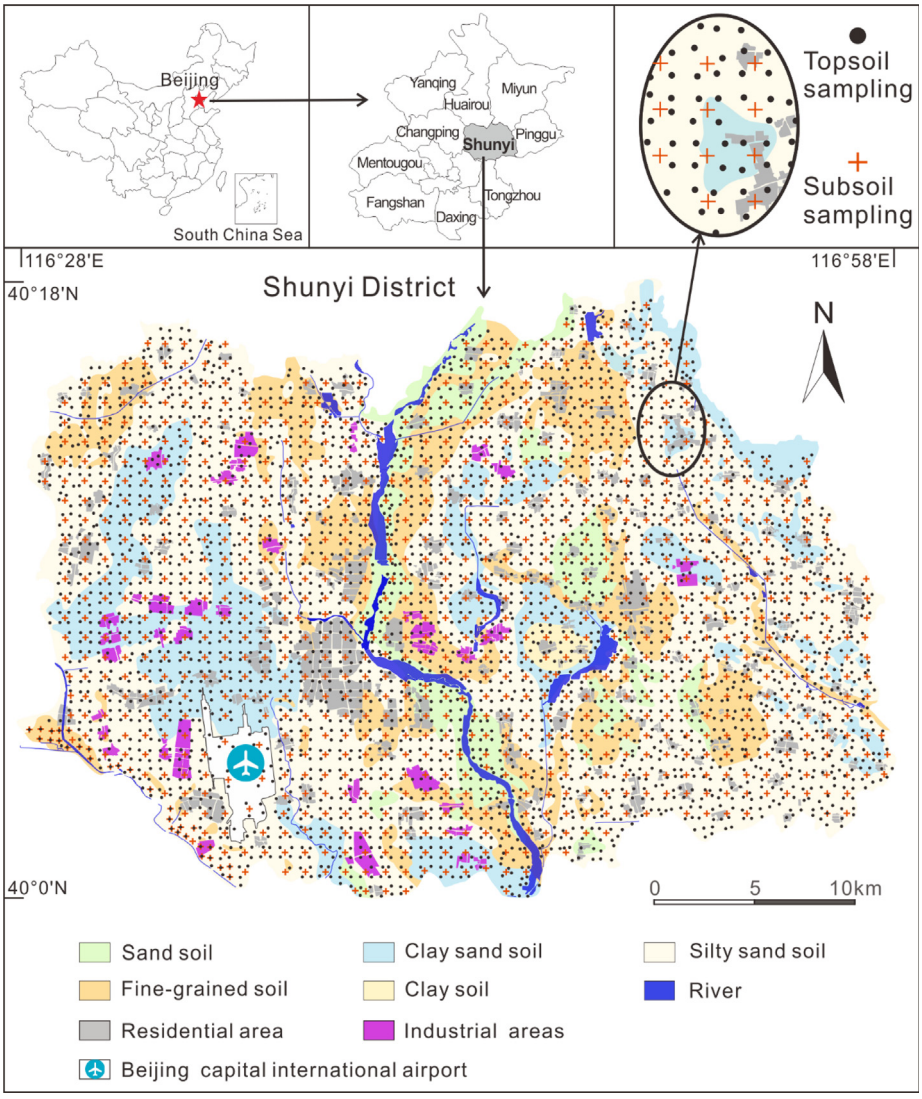

Fig. 1. Study area and location of sampling sites.

emitted from human activities (Wang et al., 2019b; Xiao et al., 2019; Zhao et al., 2014). In developing countries, the rapid economic development sharply increased anthropogenic emissions of PTEs, which would be transported atmospherically and deposited into nearby soils (Jiang et al., 2017). This may result in soil contamination at regional and even global scales. In China, a series of reports found that soils were obviously contaminated by PTEs, which increased from 185 mg/kg in 1990 to 400 mg/kg in 2015 (Chen et al., 2015; Pan et al., 2018; Zhang et al., 2018b). Over the past decades, the fast urban expansion in China has dramatically increased the industrial and municipal wastewater discharges, from 17.6 to 32.1 billion tons and 35.1 to 65.9 billion tons, respectively (Oyang and Wang, 2000; Pan et al., 2018). These sources, together with the overwhelming traffic emissions, resulted in a substantial input of PTEs into urban soils, and therefore, much attention has been paid to the urban soil contamination in some Chinese megacities (Jin et al., 2019; Liu et al., 2019; Lv and Liu, 2019). Beijing, the capital of China with a population over 20 million, is experiencing high rate of urbanization and associated soil contamination in urban areas (Chen et al., 2010; Liu et al., 2016; Wang et al., 2012), in which the PTE concentrations were detected as high at ~300 mg/kg (Chen et al., 2015). A recent study in Beijing by Yu et al. (2019) noted that a number of PTEs, including Hg, Cd, Pb, As, Zn, Cr, Ni, Co, and V would be dispersed outside with soil particles, and even be transported from urban areas to remote areas along a certain pathway. This finding may indicate that the particle-borne PTEs would be deposited into suburban soils with various distances from cities. However, few attention has been paid to PTEs in suburban soils, which may serve as a sink area for the urban emissions (Lin et al., 2017). This presents a knowledge gap regarding the impact of urban emissions on PTEs in suburban soils.

Because the human activities in suburban areas would also release PTEs, the levels and patterns of PTEs in suburban soils may not correspond to the contribution from urban transport. In Beijing, the Shunyi District is a typical suburban area. Although soils from the Shunyi District were reportedly contaminated by Beijing urban emissions (Wang et al., 2018), applications of chemical fertilizer, sewage sludge, and livestock manure for agricultural purpose would increase the soil PTE levels in this area (Luo et al., 2009; Xu and Zhang, 2017; Yang et al., 2013). In addition to the anthropogenic activities, the soil parent materials would significantly affect PTE concentrations in suburban soils as well (Guagliardi et al., 2018). However, the relative importance of rock weathering or pedogenesis to PTEs was unclear or previously neglected (Lin et al., 2017; Wang et al., 2019a).

To evaluate the various contributions to PTEs in soils, the geostatistical mapping has been used to identify the spatial features and possible sources of PTEs in soils (Li et al., 2014; Li and Feng, 2012; Men et al., 2018; Xie et al., 2011). Recently, a newly-developed method combining geostatistical analyses, multivariate analyses, redundancy analysis and robust geostatistics, has been successfully applied in

discriminating the soil PTEs inherited from rock weathering from those derived by anthropogenic sources (Lin et al., 2017; Wang et al., 2019a). This method may provide knowledge of source apportionment of PTEs in soils from the Shunyi District, and further qualify the relative contributions from different sources. It was also interesting to compare this method with a traditional source appointment method, such as positive matrix factorization (PMF) model (Lv, 2019; Lv and Liu, 2019; Zhang et al., 2018c). In this study, the goals are: (1) to investigate concentrations and spatial distributions of PTEs in topsoils and subsoils from the Shunyi district, Beijing; (2) to discriminate anthropogenic contributions from natural source of rock weathering; and (3) to apportion quantitatively the urban emission for PTEs in suburban soils.

2. Materials and methods

2.1. Study area and sampling

Our study area covers the whole area of the Shunyi District (40°00′~40°18′N, 116°28′~116°58′E, 1020 km^2) located in the northeast of Beijing. The main topography of this district is plain, with mild terrain slopes (0–3°) from north to south. The soils in the study area are comprised mainly by moisture soil (64.1%) and gray cinnamon soil (23.7%), both of which varies widely in soil textures (Fig. 1), ranging from sand soil (7.1%) and silty sand soil (50.3%) to clay soil (1.8%). The bedrock are the Jurassic-Cretaceous sandstone, consisting of the primary minerals (e.g. quartz and plagioclase) and secondary minerals (clay), which underlies the Late Quaternary sediments. The more weathered samples could be found in the center and the margin of the district, showing the relative abundances of clay and Fe_2O_3. Most of the residential houses and industrial buildings (e.g. the Jinma and Tianzhu industrial zones) are intensively distributed in the southwestern part of the Shunyi District (Fig. 1), respectively occupying 10.3% and 2.9% of the total area.

In 2012, 4127 topsoil samples (0–20 cm) and 994 subsoil samples (120–180 cm) were respectively collected in 0.25 × 0.25 km^2 grids and 1 × 1 km^2 grids from the Shunyi District, except the Capital International Airport, which is the only restricted sector with less dense sampling grids (Fig. 1). Each soil sample was passed through a 70 mesh sieve to remove stones and plant fragments. To minimize sampling errors, the samples collected from each site consisted of five sub-samples (approximately 1.0 kg each) using a stainless drill. After collection, the soil samples were stored in polyethylene bags and transported to the laboratory immediately, in which the soils were stored at 4 °C until chemical analysis.

2.2. Analytic methods and quality control

In a preliminary measurement, V, Cr, Ni, As, Cd, Zn, Pb and Hg exhibited higher contamination levels in both top- and sub-soils from the Shunyi District compared to other potentially toxic elements (PTEs). Thus, V, Cr, Ni, As, Cd, Zn, Pb and Hg were selected as indicator PTEs for distribution characteristics and source identification in this study.

Prior to chemical analysis, each soil sample (approximately 10.0 g) was air-dried and ground in an agate mortar for homogenization. Concentrations of Sc, V, Cr, Ni, As, Pb, Zn, SiO_2, Fe_2O_3, and Al_2O_3 were determined by X-ray fluorescence (XRF) spectrometry (RS-1818, HORNGJAAN). For XRF analysis, pre-treated soil samples (approximately 4.0 g) mixed with 2.0 g of boric acid were placed in the molds, and the mixtures were pressed into 32-mm diameter pellets by 9.5 MPa pressure (Li and Feng, 2012). Another portion of pre-treated samples (approximately 1.0 g) were digested in 40 ml HNO_3: HCl (2:1, v/v), and the analysis of Cd and Hg was performed by graphite furnace atomic absorption spectrophotometer (AA6810SONGPU) and atomic fluorescence spectrometry (XGY-1011A), respectively. Total content of N was measured by a micro-Kjeldhal procedure and total P by UV-2450 spectrophotometer after H_2SO_4: $HClO_4$ mixtures (1:1, v/v) digestion. For each soil sample, pH value was measured in a 1:2.5 soil: water suspension, the content of total organic carbon (TOC) was determined by dichromate oxidation of Walkley–Black.

Standard reference materials GSS-1 and GSS-4 were obtained from the Center of National Standard Reference Material of China. They were used in the quality assurance and quality control (QA/QC) procedures. Satisfied agreement was achieved between the data gained from the present results and the certified values, with recoveries between 92% and 106%. Analysis of soil samples were carried out in triplicate, and the standard deviation was within ± 5%.

2.3. Statistical analysis and geochemical mapping

Multivariate statistical analyses (SPSS 16.0) were applied to calculate the descriptive statistics (minimum, maximum, mean, median and standard deviation) and to interpret data sets. The frequency distribution of the concentration data was examined through histograms and box-plots in order to identify the type of distribution and possible outliers for each element (Lazo et al., 2019). The spatial distribution maps of the PTEs can be plotted based on the ordinary kriging interpolation in MapGis 6.7.

Principal component analysis (PCA) was performed using varimax rotation with Kaiser Normalization and interpreted in accordance with the possible origins of PTEs (Cai et al., 2015). Redundancy analysis (RDA) and associated linear models (the Canoco 5.0 software) were carried out to describe the similarity and dissimilarity in element concentrations, and provide information for the interpretation of soil properties (Vieira et al, 2018). In this method, initial data of soil parameters (TOC, pH, P, N, Fe_2O_3 and Al_2O_3), together with 8 PTE concentrations were used as the variables. Detail methods are the same as those in our recent reports (Lin et al., 2017; Wang et al., 2019a).

2.4. Quantification of the contribution to soil PTEs

In order to quantify the anthropogenic contribution of PTEs in soils, the anthropogenic contribution ratio (ACR) was calculated basing on a geochemical model as following (Bing et al., 2016). In this case, the element of Sc was selected as a reference element because it is resistant to weathering and scarcity in various pollution sources (Gao et al., 2017; Wang et al., 2019a). Herein, ACR is defined as:

$$Me_N\,(mg/kg) = Sc_S \times (Me/Sc)_B$$

$$ACR\,(\%) = 100 \times \frac{Me_T - Me_N}{Me_T}$$

$(Me/Sc)_B$ is the ratio of background value between a given metal and *Sc* (Zhang et al., 2019b); the value of Sc_s is the measured concentration in each sample; Me_T is the measured concentration of a given metal in each sample; Me_N is the rock-originated concentration of a given metal in each sample. In this case, Sc concentrations in topsoils and subsoils were at a same level (Fig. S1 of the Supplemental Materials, SM), which confirmed the resistance of Sc to natural weathering and the inheritance between topsoils and the subsoils.

Positive matrix factorization (PMF) model was used to quantify the contribution of different sources (Cao et al., 2017; Lv and Liu, 2019). In this study, PMF 5.0 software was employed to apportion the sources of PTEs in soils. Detail methods mainly followed the previous report by Cai et al. (2019b) and Zhang et al. (2018c). Briefly, estimation of the concentration uncertainty, the determination of the method detection limit and the uncertainties of variables were firstly performed, and decades model runs were subsequently conducted. After choosing a model with the lowest Q (robust) as the optimal solution, the number of factors ranging from 3 to 5 was examined by checking the Q value, the residual analysis, and the correlation between the observed and predicted values. In this case, a 3-factor solution was invariably optimal for its most stable results and reasonable factors, because the Q true value

was minimum, which is essential to control the residual matrix E and determine a reasonable number of factors (Guan et al., 2018).

2.5. Ecological risk assessment

With the aim of assessing the ecological risk, the single ecological risk index (*E(i)*) of a given PTE (Hakanson, 1980; Sun et al., 2010) is defined as:

$$E(i) = T_i \times (C_i/C_0)$$

where *Ti* is the toxic-response factor for a given PTE, which includes 40 for Hg, 30 for Cd, 10 for As, 5 for Ni and Pb, 2 for V and Cr, and 1 for Zn (Lin et al., 2017; Zhang et al., 2018a). C_i represents the PTE concentrations in soils, and C_0 is the regionally background value of PTEs in soils.

The comprehensive ecological risk index (RI) is the sum of the individual *E(i)* values. In this case, this index was applied for assessing the pollution level induced by the combination effects of 8 PTEs in soils. RI can be expressed as:

$$RI = \sum_{i=1}^{n} E(i)$$

The scale of ecological risk indicator is given in Table S1 (SM).

3. Results

3.1. Concentrations of PTEs in soils

The descriptive statistics of 8 PTE concentrations in top- and subsoil samples are summarized in Table S2. In topsoils, the mean concentrations of V, Cr, Ni, As, Cd, Zn, Pb and Hg were 68.19, 52.13, 22.91, 8.30, 0.15, 68.29, 23.84 and 0.05 mg/kg, respectively. These values were observed at similar levels compared with the background concentrations of PTEs in soils in Beijing (Table S2). In subsoils, the mean concentrations of V, Cr, Ni, As, Cd, Zn, Pb and Hg were 67.89, 52.09, 22.85, 8.25, 0.16, 69.25, 23.94 and 0.05 mg/kg, respectively (Table S2). PTE concentrations detected in top- and sub-soil samples were lower than the Grade II level listed in Chinese Soil Quality Guidelines, which were treated as standards for assessing the risks for human health (Liang et al., 2017).

Because the contributions from parent rock materials to different PTEs varied significantly, the concentrations of individual PTEs in soils may not reveal their relative enrichment or depletion. In this way, the enrichment factor (EF), defined as the ratio of the measured concentration and the background value of each element, was used to evaluate the enrichment/loss extent. Also, this factor could be utilized to assess the influence of anthropogenic source contribution on PTE enrichment in soils (Cai et al., 2019a; Harb et al., 2015). In this study, the EF values suggested the relative enrichment of V, Cr, Ni, As, and Zn in topsoils (Table S2), likely due to their massive inputs to the surface (Peng et al., 2019). Whereas higher Cd and Hg occurred in subsoils, which may be explained by the higher mobility of Hg and Cd along the soil profile as a result of their weak soil adsorption (Sayyad et al., 2010; Wang et al., 2019a; Zhang and Zheng, 2007).

Histograms and box-plots are useful tools to examine the normal distribution of elements (Lin et al., 2017). As shown in Fig. 2, the concentrations of V, Cr, Ni and As in topsoils exhibited normal distributions, reflecting the absence of considerable contributions from point source to these PTEs (Yuan et al., 2013). Due to the presence of outliers, other four elements (Cd, Zn, Pb and Hg) showed the non-normal patterns, which corresponded to samples with increased concentrations. Similar results were suggested by the box-plot (with intervals of 5%, 25%, 50%, 75% and 95%). The identified outliers which are Cd, Zn, Pb and Hg may reveal some “hot spots” associated with human emissions or mineral assemblages (Gabarrón et al., 2018; Ma et al., 2016; Yuan et al., 2013). The concentration patterns of PTEs in histograms and box-plots were similar between topsoils and subsoils (Fig. 2), which may be attributed to the same source contributions for soils at different depths.

3.2. Spatial distribution of PTEs

The spatial distribution of soil PTE concentrations reflecting the “hot spots” of PTEs is the basis of pollution evaluation and risk control (Fei et al., 2019; Sun et al., 2010). The distribution maps of 8 PTEs are shown in Fig. 3, in which the segment was divided according to 25%, 50%, 75%, 95% and 100% of concentrations. Overall, the spatial distributions of PTEs in subsoils were more homogeneous than those in topsoils. For V, Cr, Ni and As, most of the high metal concentrations were observed in the center and the northeastern part of the Shunyi District. The concentration of Fe_2O_3 and the ratio of Al_2O_3/SiO_2 also showed the similar variations within the district (Fig. 3). However, the “hot spot” sites of Cd, Zn Pb and Hg were unevenly distributed around the industrial and residential areas located in the east of the district (Fig. 1). Among these 4 PTEs, Hg could be readily volatilized from soils to air due to its volatile nature (Zhang et al., 2019a), and therefore, showed a slightly different distribution in spatial scale from other PTEs.

3.3. PCA and RDA analyses

In this study, principle component analysis (PCA) was performed for PTEs in both top- and subsoils to extract principle components, which were considered as dominant sources for PTEs (Table 1). In the Shunyi District, three extracted principle components could explained 81.6% of the total variance in both topsoils and subsoils, and probably explained the occurrence of PTEs (Yuan et al., 2013). It could be found that the PTE grouping and associated loading in topsoils were same with those in subsoils, which indicated the similar sources for PTEs in soils at different depths. Similar distributions of the factor scores of principle components suggested that the relative contributions of three factors to PTEs in subsoils may be consistent with those in topsoils (Fig. S2). A dominant loading for V, Cr, Ni and As was assigned to PC1, which explained 53.1% of the total variance of PTEs in topsoils and 42.3% in subsoils (Table 1). PC2 with high loading for Cd, Zn and Pb, occupied 17.4% and 26.0% of variance in topsoils and subsoils, respectively (Table 1). The grouping results indicated that the factor (source) responsible for the distributions of Cd, Zn and Pb was different from that for V, Cr, Ni and As. PC3 respectively occupied 11.1% and 13.3% of the total variance in top- and subsoils with high loading only for Hg (Table 1). This indicated that PC3 merely determined the occurrence and distribution of Hg.

Redundancy analysis (RDA) is an important tool to reveal the influence of soil properties on heavy metals (Gabarrón et al., 2018; Zhao et al., 2014). Due to the volatile characteristic, Hg would be readily re-volatilized from soils to air regardless of soil properties, and therefore not suitable for RDA. Other 7 PTEs and soil properties were analyzed in RDA. The results from RDA showed that soil properties (Fe_2O_3, Al_2O_3, TOC (total organic carbon), N, P and pH) (Table S3) accounted for 64.1% and 65.1% of the variance in the distributions of PTEs in topsoils and subsoils, respectively (Table S4). Among 7 PTEs topsoils, V, Cr, Ni and As were significantly correlated with Fe_2O_3 and Al_2O_3, while Cd, Zn and Pb were correlated with P, N and TOC (Fig. 4). There was no relationship between the PTE concentrations and the soil pH values.

3.4. ACR and PMF modelling

The anthropogenic contribution ratio (ACR) model has been used to calculate the anthropogenic contribution to PTEs in soils (Bing et al., 2016). The volatile Hg is not considered in ACR calculation as mentioned above. Herein, ACR value (%) stands for the proportion of anthropogenic contribution to 7 PTEs in soils. As shown in Fig. 5, the ACR

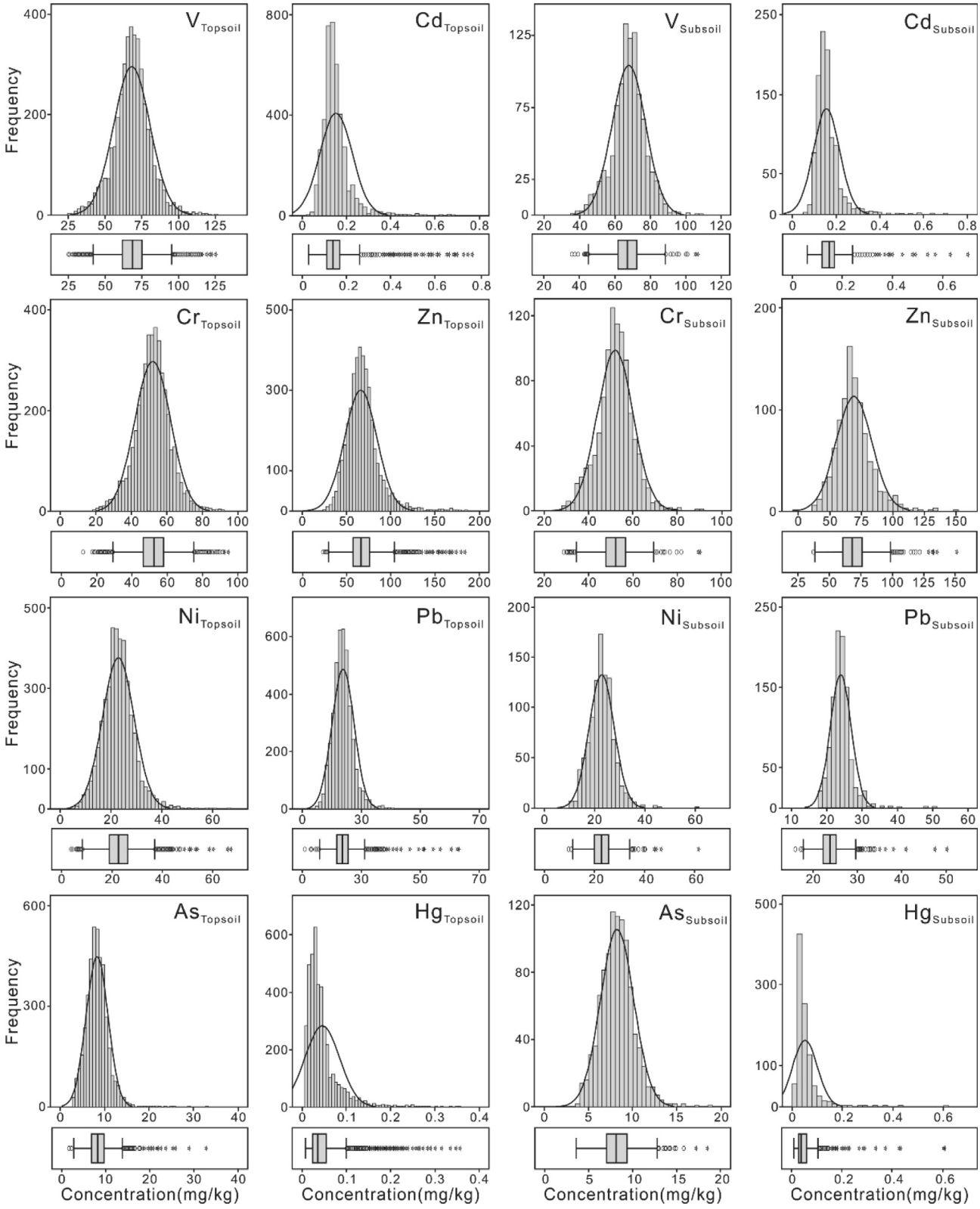

Fig. 2. Histogram and box-plot of 8 PTE concentrations in topsoils and subsoils.

distributions in topsoils showed two spatial distribution patterns, including V-Cr-Ni and As-Cd-Zn-Pb, and this clustering pattern was clearer in subsoils.

The result of source apportionment (Table S6) by positive matrix factorization (PMF) was consistent with that performed by PCA (Table 1). Therefore, three factors outputted by PMF stood for the same sources as those suggested by PCA. Furthermore, PMF provided quantitative proportions of different sources for PTEs detected in soils (Liu et al., 2018).

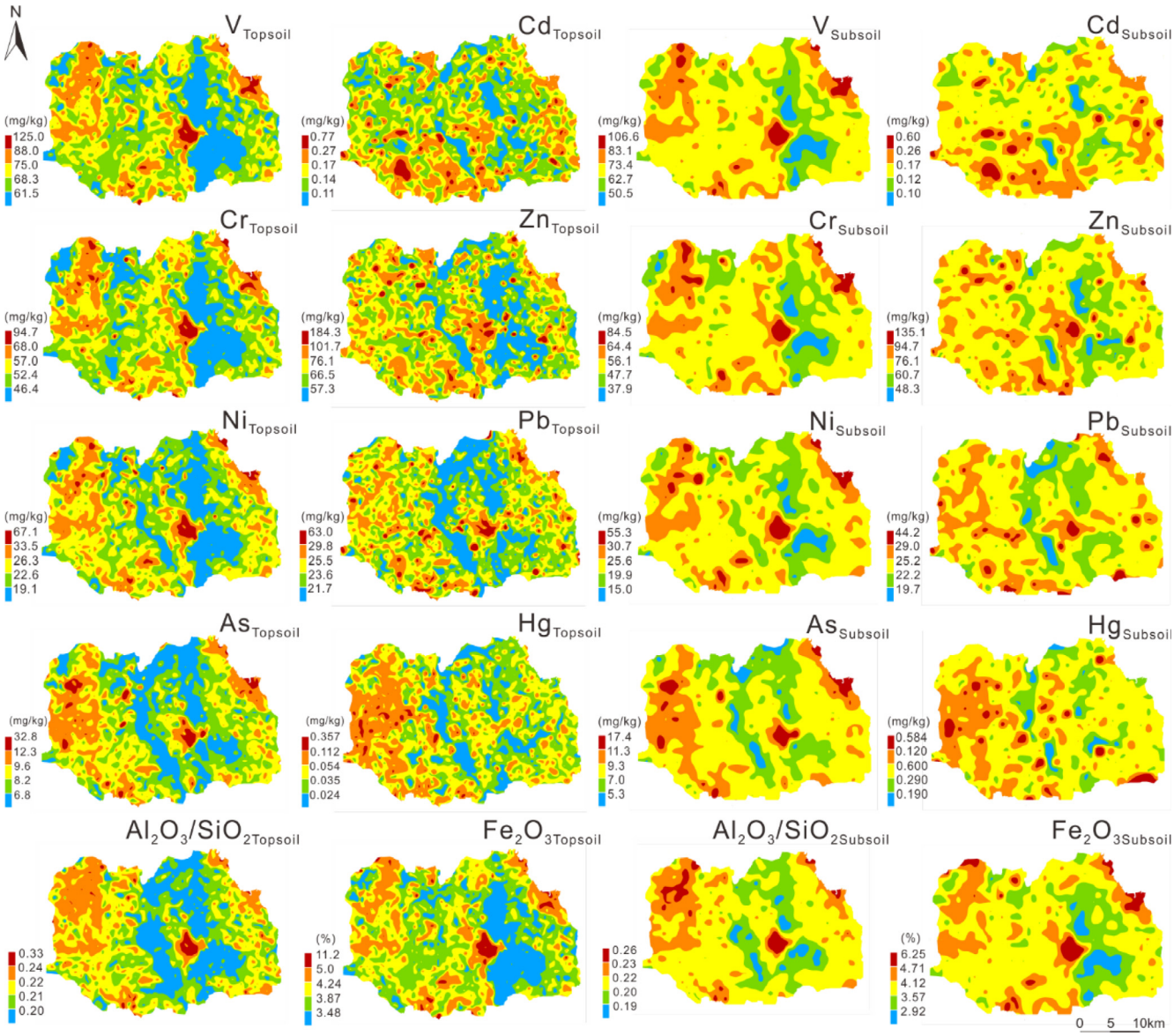

Fig. 3. Spatial distribution of 8 PTE concentrations in topsoils and subsoils.

Table 1
Factor loadings, extraction sums of squared loadings, and percentage of variance after Varimax-rotated model from PCA (n, 4127 for topsoil and 994 for subsoil).

	Topsoil			Subsoil		
	PC1	PC2	PC3	PC1	PC2	PC3
V	**0.94**	0.15	0.04	**0.94**	0.15	0.03
Cr	**0.92**	0.19	0.03	**0.92**	0.18	0.02
Ni	**0.90**	0.22	0.07	**0.90**	0.23	0.07
As	**0.77**	0.18	0.20	**0.76**	0.24	0.16
Cd	0.03	**0.89**	−0.05	0.03	**0.89**	−0.06
Zn	0.35	**0.79**	0.16	0.38	**0.75**	0.20
Pb	0.33	**0.68**	0.32	0.33	**0.74**	0.19
Hg	0.09	0.13	**0.96**	0.08	0.12	**0.98**
Eigenvalue	4.25	1.39	0.89	3.38	2.08	1.06
Variance%	53.1	17.4	11.1	42.3	26.0	13.3
Cumulative%	53.1	70.5	81.6	42.3	68.3	81.6

4. Discussion

4.1. Source interpretation

V, Cr, Ni and As were suggested to be derived from the same source and tightly associated with Fe_2O_3, Al_2O_3 through PCA/RDA analyses. As Al_2O_3, SiO_2 and Fe_2O_3 are the primary products of rock weathering, the levels of Al_2O_3/SiO_2 ratios and Fe_2O_3 concentrations are expected to reflect the degree of rock weathering or pedogenesis (Lin et al., 2017; Wang et al., 2019a). As shown in the distribution maps (Fig. 3), the high contents of soil V, Cr, Ni and As were overlapped with those of Al_2O_3/SiO_2 ratios and Fe_2O_3 concentrations in soils, particularly in subsoils. These “hot spot” sites were simultaneously covered by clay-rich soils (Fig. 1), which represent the secondary products of bedrock. This result suggested that the occurrences of V, Cr, Ni and As in soils may be resulted from the weathering process of parent soil materials. Similar results have been reported in other areas in Beijing, in which the occurrences of V, Cr, Ni and As were attributed to soil parent materials and natural processes (Li et al., 2013; Ma et al., 2016). This source contribution was further confirmed by the high concentrations of V (91.4 mg/kg), Cr (68.3 mg/kg), Ni (28.1 mg/kg) and As (12.5 mg/

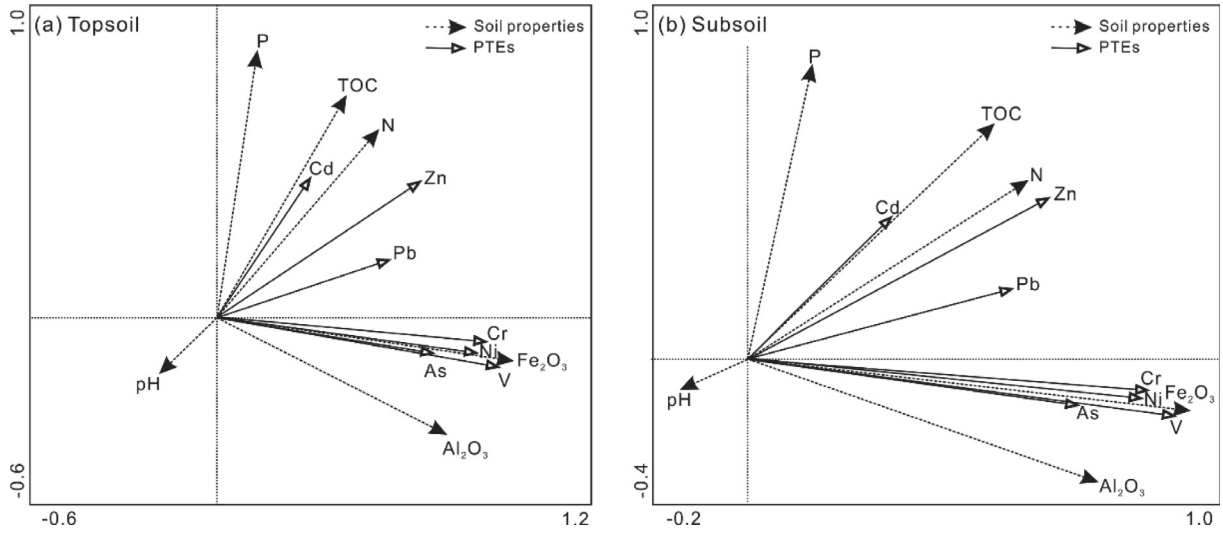

Fig. 4. Ordination biplot for PTEs and soil properties variables.

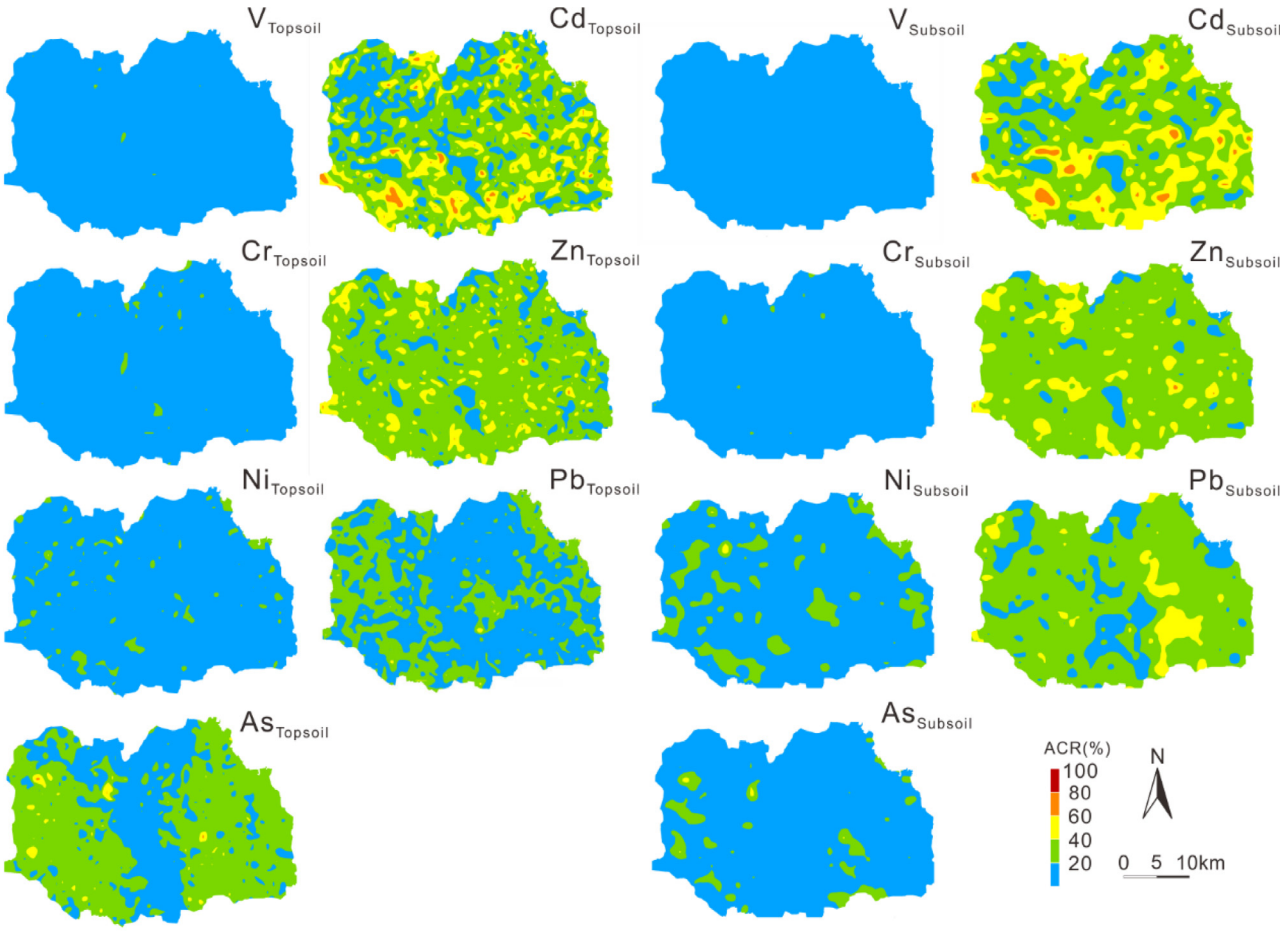

Fig. 5. Spatial distribution of anthropogenic contribution ratios to PTEs in topsoils and subsoils.

kg) found in the sandstone (NEPA, 1990), which is the bedrock in the Shunyi District. Finding from this study revealed that the natural inputs from soil parent materials dominated the occurrences of these 4 PTEs in soils. Noteworthy, the relative contribution from natural source to As was lower than that to V, Ni and Cr (Table 1), likely indicating the additional contribution from other sources (i.e. industrial emissions) to As.

For Cd, Zn, Pb and Hg, the concentration variations were irrespective of the distributions of Al_2O_3/SiO_2 ratio, Fe_2O_3 concentration, or soil texture. Previous studies in Beijing have reported that the heavy loadings of Cd, Zn Pb and Hg in soils were mainly caused by human activities (Chen et al., 2016b; Zhu et al., 2017). In this study, the result from RDA showed that the category of Cd-Zn-Pb were strongly related with organic matters (TOC, N and P) in soils (Fig. 4). Presence of N and P is widespread in both domestic as well as industrial wastewater discharges. This may suggest that the spatial variations of Cd, Zn and Pb

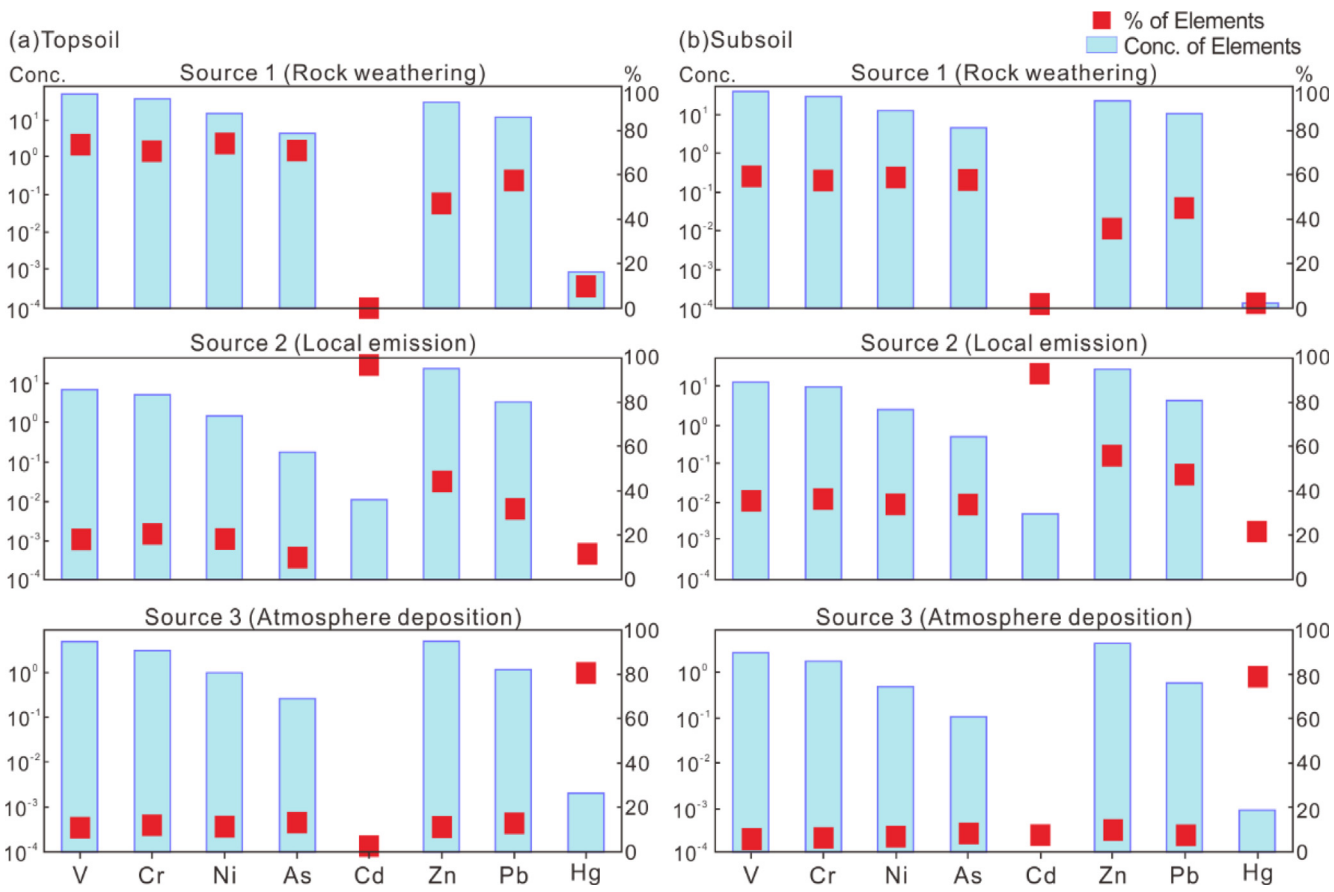

Fig. 6. Source profiles and source contributions of PTEs in topsoils (a) and subsoils (b) by PMF.

were more likely affected by local human activities, rather than rock weathering or pedogenesis. Accordingly, most of the "hot-spots" of Cd, Zn and Pb (Fig. 3) were found around the industrial and residential areas, as well as the Capital International Airport (Fig. 1). This was consistent with the results reported by Pan et al. (2016) and Zhao et al. (2014), in which a significant impact of industry on Cd, Zn and Pb levels in soils was observed. For this reason, the anthropogenic source from local emissions was the major contributor for Cd, Zn and Pb.

As shown in Fig. 3, the high-value spots for Hg were found in the west of the Shunyi District, exhibiting a different pattern from V-Cr-Ni-As or Cd-Zn-Pb. In China, elementary Hg could amount to 70% of the total Hg emission from coal combustion (Lv, 2019), and therefore, its atmospheric transport and deposition have caused Hg pollution in soils (Luo et al., 2012; Streets et al., 2005). In Beijing urban soils, high levels of Hg resulting from long-term coal combustion have been demonstrated as well (Chen et al., 2010). In particular, the winter heating was heavily dependent on coal combustion before 2008 Olympic Games (Yuan et al., 2013). Presumably, massive Hg that were released from Beijing urban areas would be transported and deposited into Shunyi soils. Thus, the atmospheric source that carried urban emissions were likely responsible for Hg in the study area. As the adsorption of Hg onto soils was lower compared to other elements, it was more readily to move downward, as well as to accumulate in subsoils (Zhang and Zheng, 2007). The usage history of coal may also explain the higher EF values of Hg in subsoils than those in topsoils (Table S2).

4.2. Quantification of source contribution

Once the dominant sources were identified for the different PTEs, the relative contributions from these sources to the distribution of PTEs could be determined by ACR modelling. Based on the estimation of ACR for all samples, the ACR distributions in topsoils showed two spatial distribution patterns, including V-Cr-Ni and As-Cd-Zn-Pb. For the V-Cr-Ni category, the ACR ratio less than 20% are of 98.9%, 97.1% and 89.6%, respectively (Table S5), with no "hot spots" observed. For the category of As-Cd-Zn-Pb, the ACR values less than 20% are of 35.8%, 32.1%, 23.0% and 58.6%, respectively (Table S5), and their "hot spots" sites (Fig. 5) corresponded to those of concentrations (Fig. 3). Compared with the ACR values of Cd, Zn and Pb, the anthropogenic loading for As was slightly lower (Table 1). In the case of As, 95.1% of ACR values are less than 40% while these values are 78.3% for Cd, 85.2% for Zn and 93.1% for Pb. In subsoils, the ACR values less than 20% are of 100%, 99.4%, 80.3% and 88.9% for V, Cr, Ni and As, respectively (Table S5), suggesting the extremely small contributions from anthropogenic activities (Fig. 5). For Cd, Zn and Pb, the ACR values more than 20% are of 65.7% and 62.1%, 76.4%, respectively, illustrating their widespreadly anthropogenic signatures in the Shunyi District.

The relative contributions from three main sources, including rock weathering, local emissions and atmospheric deposition, were quantified by PMF modelling. In topsoils, the natural source of rock weathering explained the main proportions of V (72.5%), Cr (70.7%), Ni (73.1%) and As (72.3%) (Fig. 6a). This source also contributed 46.3% of Zn, 57.2% of Pb. However, its contribution to Cd and Hg was as low at 0.3% and 7.7%, respectively. The anthropogenic source of local emissions determined the contents of Cd (96.3%), Zn (44.4%) and Pb (32.0%). The source of atmospheric deposition explained 80.2% of Hg, which was initially emitted from urban activities and subsequently deposited into suburban soils via atmospheric transport. Whereas this source contribution to other PTEs was less than 11% in topsoils. In subsoils, the contribution from natural source varied significantly among different PTEs (Fig. 6b). This source dominated the occurrences of V (59.2%), Cr (57.5%), Ni (59.0%) and As (58.7%), and contributed

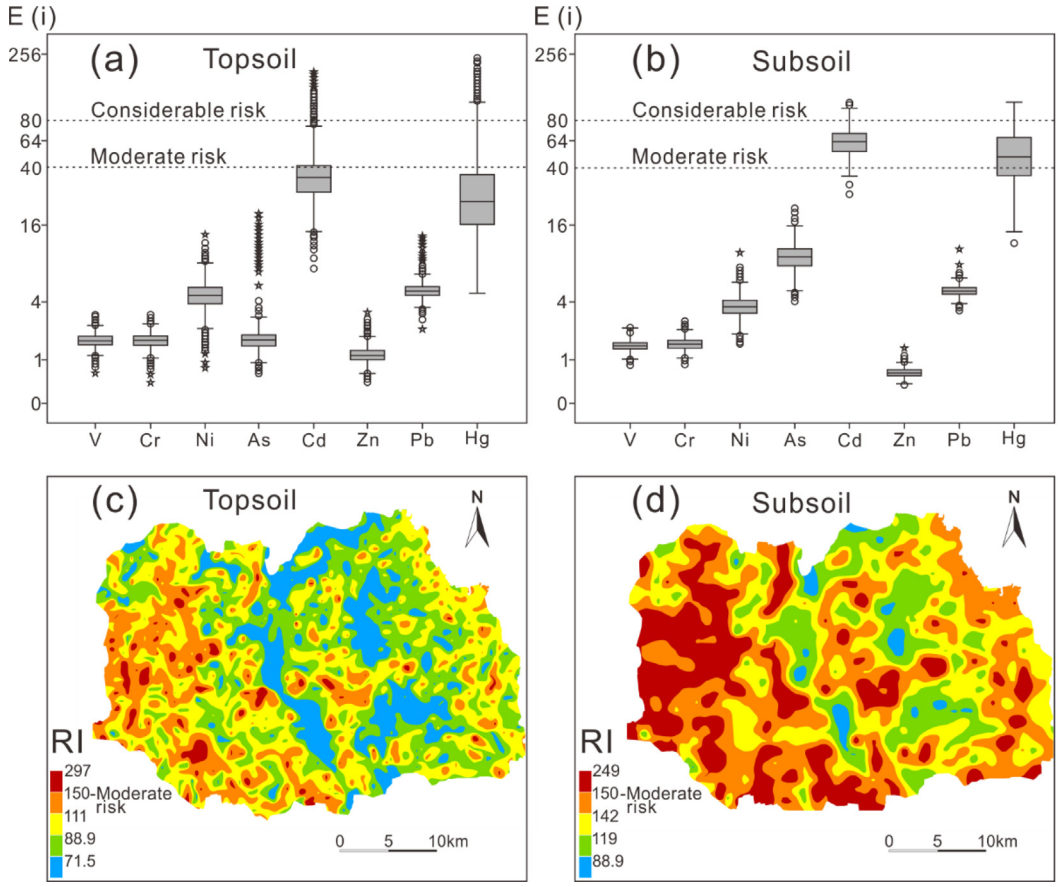

Fig. 7. Potential ecological risk factors (*E(i)*) for individual PTEs in topsoils (a) and subsoils (b), and spatial distribution of potential ecological indices (RI) for 8 PTEs in topsoils (c) and subsoils (d).

35.5% of Zn and 45.3% of Pb as well. The local emissions contributed 92.7% of Cd, 55.4% of Zn and 46.9% of Pb, and its contribution to V, Cr, Ni and As was moderate at ~30%. Similar to the case of topsoils, atmospheric deposition contributed 78.7% of Hg in subsoils while the contribution to the other PTEs was less than 10%.

Because of the occurrence of both natural and anthropogenic contributions to PTEs, the spatial variations of PTE concentrations in soils may exhibit complex interrelationships, and therefore, does not necessarily indicate the state of pollution in contrast to the cases of anthropogenic organic chemicals (e.g., chlorinated paraffins). With proper selection of data analysis methods, our study was capable of identifying the anthropogenic versus natural sources of soil PTEs across the typical suburban area. The results showed that soil Cd, Zn, Pb and Hg were more tightly associated with human activities. Because of fast industrialization and rapid urbanization, the rates of some PTE accumulation are apparently greater in China megacities and surrounding areas than elsewhere during the recent decades (Pan et al., 2018). Indeed, soil Zn and Hg concentrations in the Shunyi District have already been close to or even above moderate ecological risks based on the estimation of the ecological factors (*E(i)*) for soil PTEs (Fig. 7a and Fig. 7b). Regarding the sum of the ecological risks of 8 PTEs (RI), the high value clusters prevailed in the west of the Shunyi District, basically covering the Jinma and Tianzhu industrial zones and the Capital International Airport (Fig. 7c and d). This may reveal the significant impact of human activities on soil contamination risks, which gradually shadow the signatures of nature background (Pan et al., 2018; Peng et al., 2019). This issue is both sensitive to the government and public, and make it foremost to pinpoint the anthropogenic inputs of PTEs.

5. Conclusion

A total of 4127 top- and 994 sub-soil samples were collected from the Shunyi District, Beijing. The mean concentrations of V, Cr, Ni, As, Cd, Zn, Pb and Hg in topsoils were 68.19, 52.13, 22.91, 8.30, 0.15, 68.29, 23.84 and 0.05 mg/kg, respectively. PCA and RDA analyses demonstrated that the rock weathering was a main source of V-Cr-Ni-As in topsoils, and local emissions and atmospheric deposition were the dominant contributors for Cd-Zn-Pb and Hg, respectively. The source-PTE classification in subsoils was similar with that in topsoils, which was also demonstrated by ACR method. Results from PMF modelling suggested that rock weathering or pedogenesis contributed more than 70% of V, Cr, Ni and As in soils, local emissions contributed 92.7–96.3% of Cd, 44.4–55.4% of Zn, and 32.0–42.9% of Pb, and atmospheric source that carried urban pollutants contributed 78.7–80.2% of Hg. In this study, a series of data analysis methods including geostatistical mapping, principle component analysis, redundant analysis, anthropogenic contribution ratio and positive matrix factor were used to apportion the relative contributions of main sources to PTEs in soils. These results reveal the potentially residual capacity of PTEs, and provide solid data regarding environmental protection and pollution control.

CRediT authorship contribution statement

Xu-Chuan Duan: Software, Data curation, Writing - original draft. **Hong-Hui Yu:** Formal analysis. **Tian-Rui Ye:** Investigation, Resources. **Yong Huang:** Investigation. **Jun Li:** Investigation, Visualization. **Guo-Li Yuan:** Supervision, Conceptualization, Methodology, Writing - review & editing. **Stefano Albanese:** Software, Validation.

Declaration of Competing Interest

The authors declare that they have no known competing financial interests or personal relationships that could have appeared to influence the work reported in this paper.

Acknowledgments

This study was financially supported by the National Natural Science Foundation of China (41872100, 41372249) and the Fundamental Research Funds for the Central Universities (2652018160, 2652018158). We sincerely thank the project members from Beijing Institute of Geo-exploration Technology for their help in collecting the samples.

Appendix A. Supplementary data

Supplementary data to this article can be found online at https://doi.org/10.1016/j.ecolind.2020.106085.

References

Akinwunmi, F., Akinhanmi, T.F., Atobatele, Z.A., Adewole, O., Odekunle, K., Arogundade, L.A., Odukoya, O.O., Olayiwola, O.M., Ademuyiwa, O., 2017. Heavy metal burdens of public primary school children related to playground soils and classroom dusts in Ibadan North-West local government area, Nigeria. Environ. Toxicol. Pharmacol. 49, 21–26.

Bing, H., Wu, Y., Zhou, J., Li, R., Wang, J., 2016. Historical trends of anthropogenic metals in Eastern Tibetan Plateau as reconstructed from alpine lake sediments over the last century. Chemosphere 148, 211–219.

Cai, L.M., Xu, Z.C., Bao, P., He, M., Dou, L., Chen, L.G., Zhou, Y.Z., Zhu, Y.G., 2015. Multivariate and geostatistical analyses of the spatial distribution and source of arsenic and heavy metals in the agricultural soils in Shunde, Southeast China. J. Geochem. Explor. 148, 189–195.

Cai, L.M., Wang, Q.S., Wen, H.H., Luo, J., Wang, S., 2019a. Heavy metals in agricultural soils from a typical township in Guangdong Province, China: occurrences and spatial distribution. Ecotoxicol. Environ. Saf. 168, 184–191.

Cai, L.M., Jiang, H.H., Luo, J., 2019b. Metals in soils from a typical rapidly developing county, Southern China: levels, distribution, and source apportionment. Environ. Sci. Pollut. Res. 26, 19283–19293.

Cao, H., Chao, S., Qiao, L., Jiang, Y., Zeng, X., Fan, X., 2017. Urbanization-related changes in soil PAHs and potential health risks of emission sources in a township in Southern Jiangsu, China. Sci. Total Environ. 575, 692–700.

Chen, H., Teng, Y., Lu, S., Wang, Y., Wang, J., 2015. Contamination features and health risk of soil heavy metals in China. Sci. Total Environ. 512, 143–153.

Chen, H., Teng, Y., Lu, S., Wang, Y., Wu, J., Wang, J., 2016a. Source apportionment and health risk assessment of trace metals in surface soils of Beijing metropolitan, China. Chemosphere 144, 1002–1011.

Chen, X., Xia, X., Wu, S., Wang, F., Guo, X., 2010. Mercury in urban soils with various types of land use in Beijing, China. Environ. Pollut. 158, 48–54.

Chen, X.M., Ji, H.B., Yang, W., Zhu, B.H., Ding, H.J., 2016b. Speciation and distribution of mercury in soils around gold mines located upstream of Miyun Reservor, Beijing, China. J. Geochem. Explor. 163, 1–9.

Cortada, U., Hidalgo, M.C., Martínez, J., Rey, J., 2018. Impact in soils caused by metal (loid) s in lead metallurgy. The case of La Cruz Smelter (Southern Spain). J. Geochem. Explor. 190, 302–313.

Fei, X., Xiao, R., Christakos, G., Langousis, A., Ren, Z., Tian, Y., Lv, X., 2019. Comprehensive assessment and source apportionment of heavy metals in Shanghai agricultural soils with different fertility levels. Ecol. Indic. 106, 105508.

Gao, L., Wang, Z., Shan, J., Chen, J., Tang, C., Yi, M., 2017. Aquatic environmental changes and anthropogenic activities reflected by the sedimentary records of the Shima River, Southern China. Environ. Pollut. 224, 70–81.

Gabarrón, M., Faz, A., Acosta, J.A., 2018. Use of multivariable and redundancy analysis to assess the behavior of metals and arsenic in urban soil and road dust affected by metallic mining as a base for risk assessment. J. Environ. Manage. 206, 192–201.

Gbadamosi, M.R., Afolabi, T.A., Ogunneye, A.L., Ogunbanjo, O.O., Omotola, E.O., Kadiri, T.M., Akinsipo, O.B., Jegede, D.O., 2018. Distribution of radionuclides and heavy metals in the bituminous sand deposit in Ogun State, Nigeria–a multi-dimensional pollution, health and radiological risk assessment. J. Geochem. Explor. 190, 187–199.

Guagliardi, I., Cicchella, D., De Rosa, R., Ricca, N., Buttafuoco, G., 2018. Geochemical sources of vanadium in soils: evidences in a southern Italy area. J. Geochem. Explor. 184, 358–364.

Guan, Q., Wang, F., Xu, C., Pan, N., Lin, J., Zhao, R., Yang, Y., Luo, H., 2018. Source apportionment of heavy metals in agricultural soil based on PMF: a case study in Hexi Corridor, northwest China. Chemosphere 193, 189–197.

Hakanson, L., 1980. An ecological risk index for aquatic pollution control. A sedimentological approach. Water Res. 14, 975–1001.

Harb, M.K., Ebqa'Ai, M., Al-Rashidi, A., Alaziqi, B.H., Rashidi, M.S.A., Ibrahim, B., 2015. Investigation of selected heavy metals in street and house dust from Al-Qunfudah, Kingdom of Saudi Arada. Environ. Earth Sci. 74, 1755–1763.

Jiang, Y., Chao, S., Liu, J., Yang, Y., Chen, Y., Zhang, A., Cao, H., 2017. Source apportionment and health risk assessment of heavy metals in soil for a township in Jiangsu Province, China. Chemosphere 168, 1658–1668.

Jin, Y., O'Connor, D., Ok, Y.S., Tsang, D.C., Liu, A., Hou, D., 2019. Assessment of sources of heavy metals in soil and dust at children's playgrounds in Beijing using GIS and multivariate statistical analysis. Environ. Int. 124, 320–328.

Keesing, F., Belden, L.K., Daszak, P., Dobson, A., Harvell, C.D., Holt, R.D., Hudson, P., Jolles, A., Jones, K.E., Mitchell, C.E., Myers, S.S., 2010. Impacts of biodiversity on the emergence and transmission of infectious diseases. Nature 468, 647.

Khan, S., Cao, Q., Zheng, Y.M., Huang, Y.Z., Zhu, Y.G., 2008. Health risks of heavy metals in contaminated soils and food crops irrigated with wastewater in Beijing, China. Environ. Pollut. 152, 686–692.

Lazo, P., Stafilov, T., Qarri, F., Allajbeu, S., Bekteshi, L., Frontasyeva, M., Harmens, H., 2019. Spatial distribution and temporal trend of airborne trace metal deposition in Albania studied by moss biomonitoring. Ecol. Indic. 101, 1007–1017.

Li, W., Xu, B., Song, Q., Liu, X., Xu, J., Brookes, P.C., 2014. The identification of 'hotspots' of heavy metal pollution in soil-rice systems at a regional scale in eastern China. Sci. Total Environ. 472, 407–420.

Li, X., Feng, L., 2012. Multivariate and geostatistical analyzes of metals in urban soil of Weinan industrial areas, Northwest of China. Atmos. Environ. 47, 58–65.

Li, X., Liu, L., Wang, Y., Luo, G., Chen, X., Yang, X., Hall, M.H.P., Guo, R., Wang, H., Cui, J., He, X., 2013. Heavy metal contamination of urban soil in an old industrial city (Shenyang) in Northeast China. Geoderma 192, 50–58.

Liang, J., Feng, C., Zeng, G., Gao, X., Zhong, M., Li, X., Li, X., He, X., Fang, Y., 2017. Spatial distribution and source identification of heavy metals in surface soils in a typical coal mine city, Lianyuan, China. Environ. Pollut. 225, 681–690.

Lin, Y., Han, P., Huang, Y., Yuan, G.L., Guo, J.X., Li, J., 2017. Source identification of potentially hazardous elements and their relationships with soil properties in agricultural soil of the Pinggu district of Beijing, China: multivariate statistical analysis and redundancy analysis. J. Geochem. Explor. 173, 110–118.

Liu, E., Wang, X., Liu, H., Liang, M., Zhu, Y., Li, Z., 2019. Chemical speciation, pollution and ecological risk of toxic metals in readily washed off road dust in a megacity (Nanjing), China. Ecotoxicol. Environ. Saf. 173, 381–392.

Liu, J., Chen, Y., Chao, S., Cao, H., Zhang, A., Yang, Y., 2018. Emission control priority of PM2.5-bound heavy metals in different seasons: a comprehensive analysis from health risk perspective. Sci. Total Environ. 644, 20–30.

Liu, R., Wang, M., Chen, W., Peng, C., 2016. Spatial pattern of heavy metals accumulation risk in urban soils of Beijing and its influencing factors. Environ. Pollut. 210, 174–181.

Luo, L., Ma, Y., Zhang, S., Wei, D., Zhu, Y.G., 2009. An inventory of trace element inputs to agricultural soils in China. J. Environ. Manage. 90, 2524–2530.

Luo, X.S., Yu, S., Zhu, Y.G., Li, X.D., 2012. Trace metal contamination in urban soils of China. Sci. Total Environ. 421–422, 17–30.

Lv, J., 2019. Multivariate receptor models and robust geostatistics to estimate source apportionment of heavy metals in soils. Environ. Pollut. 244, 72–83.

Lv, J., Liu, Y., 2019. An integrated approach to identify quantitative sources and hazardous areas of heavy metals in soils. Sci. Total Environ. 646, 19–28.

Lv, J., Liu, Y., Zhang, Z., Dai, B., 2014. Multivariate geostatistical analyses of heavy metals in soils: Spatial multi-scale variations in Wulian, Eastern China. Ecotoxicol. Environ. Saf. 107, 140–147.

Ma, Z., Chen, K., Li, Z., Bi, J., Huang, L., 2016. Heavy metals in soils and road dusts in the mining areas of Western Suzhou, China: a preliminary identification of contaminated sites. J. Soils Sediments 16, 204–214.

Men, C., Liu, R., Xu, F., Wang, Q., Guo, L., Shen, Z., 2018. Pollution characteristics, risk assessment, and source apportionment of heavy metals in road dust in Beijing, China. Sci. Total Environ. 612, 138–147.

National Environmental Protection Agency (NEPA), 1990. The Background Values of Soil Elements of China. Chinese Environmental Science Press, Beijing (in Chinese).

Oyang, Z., Wang, R., 2000. Water environmental problems and ecological options in China. In China water vision: Meeting the water challenge in rapid transition. The 2nd world water forum, The Hague (pp. 17-22).

Pan, L., Ma, J., Wang, X., Hou, H., 2016. Heavy metals in soils from a typical county in Shanxi Province, China: levels, sources and spatial distribution. Chemosphere 148, 248–254.

Pan, L., Wang, Y., Ma, J., Hu, Y., Su, B., Fang, G., Wang, L., Xiang, B., 2018. A review of heavy metal pollution levels and health risk assessment of urban soils in Chinese cities. Environ. Sci. Pollut. Res. 25, 1055–1069.

Peng, H., Chen, Y., Weng, L., Ma, J., Ma, Y., Li, Y., Shafiqul Islam, M., 2019. Comparisons of heavy metal input inventory in agricultural soils in North and South China: a review. Sci. Total Environ. 660, 776–786.

Ravankhah, N., Mirzaei, R., Masoum, S., 2017. Determination of heavy metals in surface soils around the brick kilns in an arid region, Iran. J. Geochem. Explor. 176, 91–99.

Sayyad, G., Afyuni, M., Mousavi, S.F., Abbaspour, K.C., Richards, B.K., Schulin, R., 2010. Transport of Cd, Cu, Pb and Zn in a calcareous soil under wheat and safflower cultivation—a column study. Geoderma 154, 311–320.

Streets, D.G., Hao, J., Wu, Y., Jiang, J., Chan, M., Tian, H., Feng, X., 2005. Anthropogenic mercury emissions in China. Atmos. Environ. 39, 7789–7806.

Sun, Y.B., Zhou, Q.X., Xie, X.K., Liu, R., 2010. Spatial, sources and risk assessment of heavy metal contamination of urban soil in typical regions of Shenyang, China. J. Hazard. Mater. 174, 455–462.

Tóth, G., Hermann, T., Da Silva, M.R., Montanarella, L., 2016. Heavy metals in agricultural soils of the European Union with implications for food safety. Environ. Int. 88, 299–309.

Vieira, L.R., Morgado, F., Nogueira, A.J., Soares, A.M., Guilhermino, L., 2018. Integrated multivariate approach of ecological and ecotoxicological parameters in coastal

environmental monitoring studies. Ecol. Indic. 95, 1128–1142.
Wang, A.T., Wang, Q., Li, J., Yuan, G.L., Albanese, S., Petrik, A., 2019a. Geo-statistical and multivariate analyses of potentially toxic elements' distribution in the soil of Hainan Island (China): a comparison between the topsoil and subsoil at a regional scale. J. Geochem. Explor. 197, 48–59.
Wang, M., Bai, Y., Chen, W., Markert, B., Peng, C., Ouyang, Z., 2012. A GIS technology based potential eco-risk assessment of metals in urban soils in Beijing, China. Environ. Pollut. 161, 235–242.
Wang, M., Liu, R., Chen, W., Peng, C., Markert, B., 2018. Effects of urbanization on heavy metal accumulation in surface soils, Beijing. J. Environ. Sci. 64, 328–334.
Wang, S., Cai, L.M., Wen, H.H., Luo, J., Wang, Q.S., Liu, X., 2019b. Spatial distribution and source apportionment of heavy metals in soil from a typical county-level city of Guangdong Province, China. Sci. Total Environ. 655, 92–101.
Xiao, R., Guo, D., Ali, A., Mi, S., Liu, T., Ren, C., Li, R., Zhang, Z., 2019. Accumulation, ecological-health risks assessment, and source apportionment of heavy metals in paddy soils: a case study in Hanzhong, Shaanxi, China. Environ. Pollut. 248, 349–357.
Xie, Y., Chen, T.B., Lei, M., Yang, J., Guo, Q.J., Song, B., Zhou, X.Y., 2011. Spatial distribution of soil heavy metal pollution estimated by different interpolation methods: accuracy and uncertainty analysis. Chemosphere 82, 468–476.
Xu, Q., Zhang, M., 2017. Source identification and exchangeability of heavy metals accumulated in vegetable soils in the coastal plain of eastern Zhejiang province, China. Ecotoxicol. Environ. Saf. 142, 410–416.
Yang, S., Zhou, D., Yu, H., Wei, R., Pan, B., 2013. Distribution and speciation of metals (Cu, Zn, Cd, and Pb) in agricultural and non-agricultural soils near a stream upriver from the Pearl River, China. Environ. Pollut. 177, 64–70.
Yu, G., Qin, X., Xu, J., Zhou, Q., Wang, B., Huang, K., Deng, C., 2019. Characteristics of particulate-bound mercury at typical sites situated on dust transport paths in China. Sci. Total Environ. 648, 1151–1160.
Yuan, G.L., Sun, T.H., Han, P., Li, J., 2013. Environmental geochemical mapping and multivariate geostatistical analysis of heavy metals in topsoils of a closed steel smelter: capital Iron & Steel Factory, Beijing, China. J. Geochem. Explor. 130, 15–21.
Zhang, H., Wang, Z.W., Zhang, X.S., 2019a. Methylmercury concentrations and potential sources in atmospheric fine particles in Beijing, China. Sci. Total Environ. 681, 183–190.
Zhang, M.K., Zheng, S.A., 2007. Competitive adsorption of Cd, Cu, Hg and Pb by agricultural soils of the Changjiang and Zhujiang deltas in China. J. Zhejiang Univ-Sc. A 8, 1808–1815.
Zhang, P., Qin, C., Hong, X., Kang, G., Qin, M., Yang, D., Pang, B., Li, Y., He, J., Dick, R.P., 2018a. Risk assessment and source analysis of soil heavy metal pollution from lower reaches of Yellow River irrigation in China. Sci. Total Environ. 633, 1136–1147.
Zhang, X., Zha, T., Guo, X., Meng, G., Zhou, J., 2018b. Spatial distribution of metal pollution of soils of Chinese provincial capital cities. Sci. Total Environ. 643, 1502–1513.
Zhang, X., Wei, S., Sun, Q., Wadood, S.A., Guo, B., 2018c. Source identification and spatial distribution of arsenic and heavy metals in agricultural soil around Hunan industrial estate by positive matrix factorization model, principle components analysis and geo statistical analysis. Ecotoxicol. Environ. Saf. 159, 354–362.
Zhang, Z., Zheng, D., Xue, Z., Wu, H., Jiang, M., 2019b. Identification of anthropogenic contributions to heavy metals in wetland soils of the Karuola Glacier in the Qinghai-Tibetan Plateau. Ecol. Indic. 98, 678–685.
Zhao, L., Xu, Y., Hou, H., Shangguan, Y., Li, F., 2014. Source identification and health risk assessment of metals in urban soils around the Tanggu chemical industrial district, Tianjin, China. Sci. Total Environ. 468–469, 654–662.
Zhu, G., Guo, Q., Xiao, H., Chen, T., Yang, J., 2017. Multivariate statistical and lead isotopic analyses approach to identify heavy metal sources in topsoil from the industrial zone of Beijing Capital Iron and Steel Factory. Environ. Sci. Pollut. Res. 24, 14877–14888.